CANCER

Neoantigen responses, immune correlates, and favorable outcomes after ipilimumab treatment of patients with prostate cancer

Sumit K. Subudhi[1], Luis Vence[2], Hao Zhao[2], Jorge Blando[2], Shalini S. Yadav[2], Qing Xiong[2], Alexandre Reuben[3], Ana Aparicio[1], Paul G. Corn[1], Brian F. Chapin[4], Louis L. Pisters[4], Patricia Troncoso[5], Rebecca Slack Tidwell[6], Peter Thall[6], Chang-Jiun Wu[7], Jianhua Zhang[7], Christopher L. Logothetis[1], Andrew Futreal[7], James P. Allison[2,8†], Padmanee Sharma[1,2,8*†]

Tumors with high mutational burden (TMB) tend to be responsive to immune checkpoint blockade (ICB) because there are neoantigens available for targeting by reinvigorated T cells, whereas those with low TMB demonstrate limited clinical responses. To determine whether antigen-specific T cell responses can be elicited after treatment with ICB in cancers that have a low TMB, we conducted a clinical trial with ipilimumab in 30 patients with metastatic castration-resistant prostate cancer. We identified two distinct cohorts by survival and progression times: "favorable" (*n* = 9) and "unfavorable" (*n* = 10). Patients in the favorable cohort had high intratumoral CD8 T cell density and IFN-γ response gene signature and/or antigen-specific T cell responses. Two patients with a relatively low TMB had T cell responses against unique neoantigens. Moreover, six of nine patients in the favorable group are still alive at the time of analysis, with survival ranging from 33 to 54 months after treatment. All 10 patients in the unfavorable cohort have succumbed to their disease and had survival ranging from 0.6 to 10.3 months. Collectively, our data indicate that immunological correlates associated with effector T cell responses are observed in patients with metastatic prostate cancer who benefit from ICB.

INTRODUCTION

Immune checkpoint blockade (ICB) has revolutionized the therapeutic landscape of clinical oncology by inducing durable T cell–mediated antitumor responses in patients with advanced malignancies. Despite the unprecedented successes of ICB, only a subset of patients with cancer derives clinical benefit. Some of the highest objective response rates to ICB are observed in patients with melanoma and non–small cell lung cancer (NSCLC), tumors that have high tumor mutational burden (TMB) and neoantigen frequency (*1*), both of which have been associated with clinical responses to ICB (*2*–*5*). Because tumor neoantigens can be recognized by the immune system (*6*), it is expected that the presence of preexisting immune infiltrates within the tumor microenvironment is also associated with clinical benefit to ICB (*7*, *8*). In comparison to melanoma and NSCLC, prostate cancers have a substantially lower prevalence of somatic mutations and frequency of mutant neoantigens (*1*). Although targeting the immune checkpoint molecule cytotoxic T lymphocyte–associated antigen 4 (CTLA-4) with ipilimumab in patients with metastatic castration-resistant prostate cancer (mCRPC) failed to demonstrate a survival benefit in two phase 3 clinical trials (*9*, *10*), there was a subset of men who derived significant durable clinical responses after treatment with ipilimumab (*10*, *11*). Here, we report clinical outcomes from a trial designed to test the hypothesis that induction of an effective antitumor response by ipilimumab may be mediated, at least in part, by T cell responses to cancer neoantigens in patients with mCRPC.

RESULTS

Phase 2 clinical trial of ipilimumab in mCRPC

To evaluate systemic T cell responses against cancer neoantigens after treatment with ipilimumab, 30 patients with mCRPC were

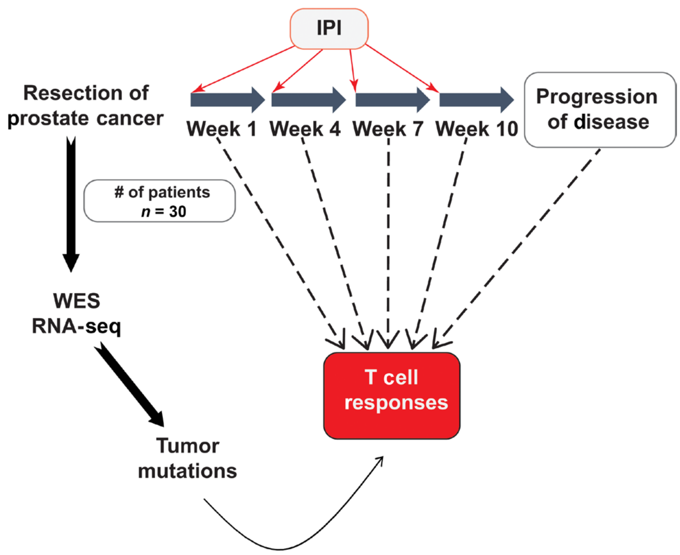

Fig. 1. Clinical trial schema. IPI, ipilimumab; WES, whole-exome sequencing; RNA-seq, RNA sequencing.

[1]Department of Genitourinary Medical Oncology, University of Texas MD Anderson Cancer Center, Houston, TX 77030, USA. [2]Immunotherapy Platform, University of Texas MD Anderson Cancer Center, Houston, TX 77030, USA. [3]Department of Thoracic Head and Neck Medical Oncology, University of Texas MD Anderson Cancer Center, Houston, TX 77030, USA. [4]Department of Urology, University of Texas MD Anderson Cancer Center, Houston, TX 77030, USA. [5]Department of Pathology, University of Texas MD Anderson Cancer Center, Houston, TX 77030, USA. [6]Department of Biostatistics, University of Texas MD Anderson Cancer Center, Houston, TX 77030, USA. [7]Department of Genomic Medicine, University of Texas MD Anderson Cancer Center, Houston, TX 77030, USA. [8]Department of Immunology, The University of Texas MD Anderson Cancer Center, Houston, TX 77030, USA.
*Corresponding author. Email: padsharma@mdanderson.org
†These authors contributed equally to this work.

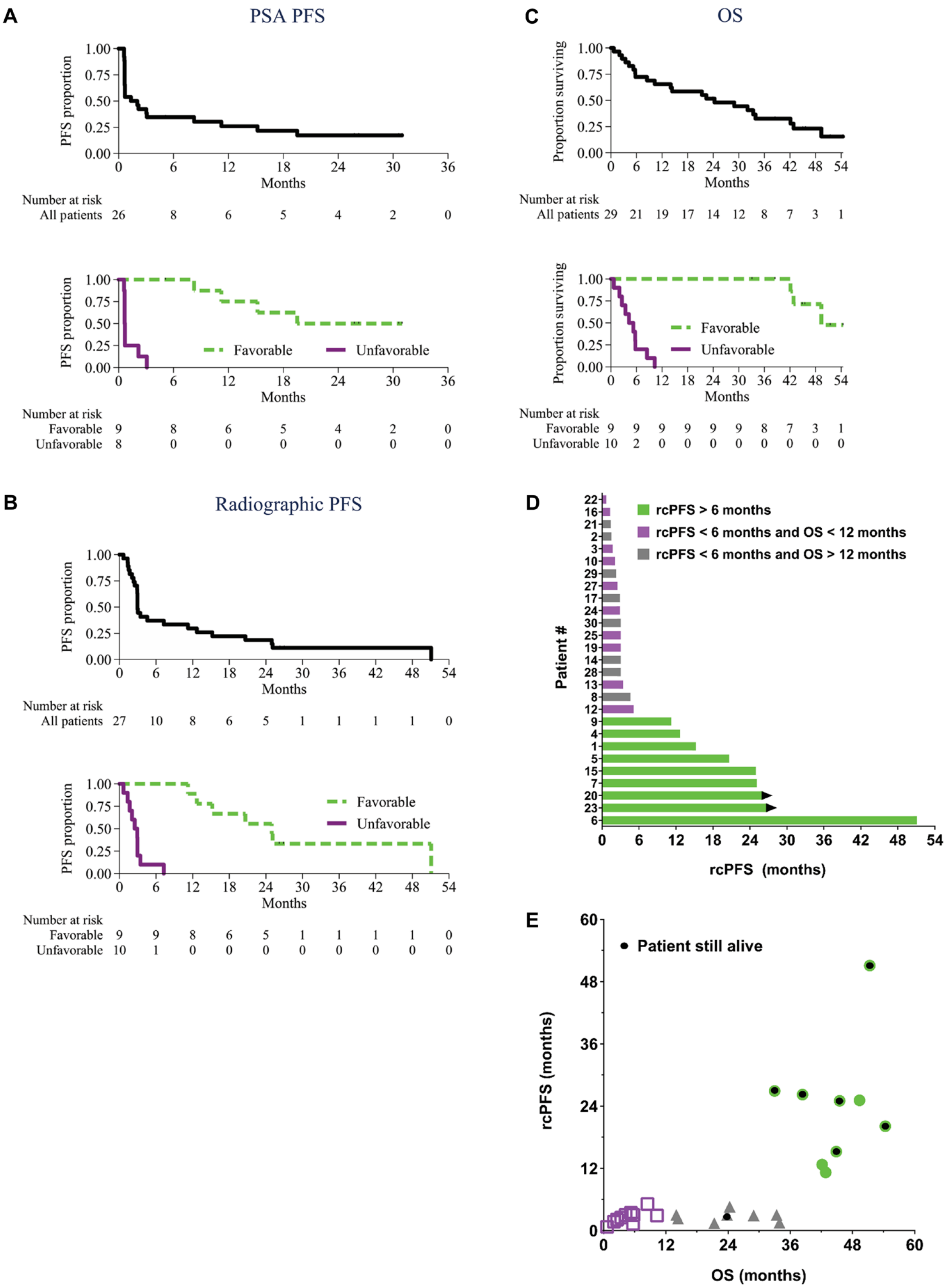

Fig. 2. Clinical outcomes of patients with metastatic prostate cancer treated with ipilimumab. (**A**) Patients were stratified into response cohorts based on composite of radiographic/clinical progression-free survival (rcPFS) and overall survival (OS). PSA PFS for total cohort (top; $n = 26$) and favorable ($n = 9$) and unfavorable ($n = 8$) cohorts (bottom) were estimated by the Kaplan-Meier method. (**B**) Radiographic PFS for total cohort (top; $n = 27$) and favorable ($n = 9$) and unfavorable ($n = 10$) cohorts (bottom) were estimated by the Kaplan-Meier method. (**C**) OS for total cohort (top; $n = 29$) and favorable ($n = 9$) and unfavorable ($n = 10$) cohorts (bottom) were estimated by the Kaplan-Meier method. (**D**) Composite of rcPFS. Each bar represents an individual patient ($n = 27$). Black arrows denote patients who are having ongoing responses. The favorable cohort is depicted by green bars ($n = 9$), the unfavorable cohort is depicted by purple bars ($n = 10$), and the remaining patients are depicted by gray bars ($n = 8$). (**E**) The favorable cohort is represented by green closed circles ($n = 9$), the unfavorable cohort is represented by purple open squares ($n = 10$), and the remaining patients are represented by gray closed triangles ($n = 8$). Black dots represent patients who are still alive.

enrolled into a single center study (NCT02113657) from January 2015 to May 2018 (Fig. 1). Twenty-nine (97%) patients received at least one dose of ipilimumab (3 mg/kg per dose, every 3 weeks for up to four doses), and they were evaluated for safety and efficacy; however, two patients withdrew consent after initiating treatment and were not included in the correlative analyses. The baseline characteristics, metastatic distribution, and prior systemic therapies for mCRPC of the 29 patients are described in tables S1, S2, and S3, respectively.

Safety and efficacy

Evaluation of clinical safety, tolerability, and serum prostate-specific antigen (PSA) kinetics after treatment with ipilimumab were some of the key clinical objectives of this trial. Median follow-up time from the administration of the first dose of ipilimumab was 45.5 months. Eleven (38%) of 29 patients received all four doses of ipilimumab, and the median number of doses received was three (interquartile range, 2 to 4). Eight (28%) patients developed grade 3 toxicities attributed to treatment. Similar to other prostate cancer trials with ipilimumab (*9*–*15*), the most common grade 3 immune-related adverse events (irAEs) were dermatitis (10%) and diarrhea (10%; table S4). No grade 4 or 5 toxicities were observed.

The median PSA progression-free survival (PFS) time was 1.7 months [95% confidence interval (CI) (0.7, 8.2 months); Fig. 2A], median radiographic PFS was 3.0 months [95% CI (2.5, 11.2 months); Fig. 2B], and median overall survival (OS) time was 24.3 months [95% CI (8.5, 33.9 months); Fig. 2C] with 22 (76%) patients having succumbed to their disease. The best overall radiographic response observed in this study was stable disease, and the disease control rate (DCR) was 37% for this cohort of patients.

There were two predominant categories of radiographic and/or clinical PFS (rcPFS; whichever occurred first): (i) those with rcPFS >6 months (n = 9) and (ii) those with rcPFS <6 months (n = 18; Fig. 2D). All patients with rcPFS >6 months also had an OS >12 months, which we characterized as clinical benefit, and they were deemed the "favorable" cohort (n = 9) for subsequent correlative studies. The remaining 18 patients had rcPFS <6 months, which were further segregated by OS [<12 months (n = 10); >12 months (n = 8); Fig. 2E]. Patients with PFS <6 months and OS <12 months

Table 1. Clinical outcomes for the favorable cohort. Blue font indicates that the patients are having ongoing responses. SD, stable disease. NS, nonsynonymous.

Patient #	# NS mutations	PSA PFS (months)	Radiographic PFS (months)	Best overall response	OS (months)
1	41	15.2	15.2	SD	44.9
4	708	8.2	12.7	SD	42.2
5	24	19.5	20.6	SD	54.3
6	2	5.1*	51.1	SD	51.4
7	13	25.7*	25.1	SD	49.4
9	25	11.2	11.2	SD	42.8
15	104	30.6*	25.0	SD	45.5
20	31	26.2	26.2	SD	38.4
23	25	30.9	26.9	SD	33.0

*The patient started abiraterone acetate before developing PSA progression.

Table 2. Clinical outcomes for the unfavorable cohort. na, not available. For patients na for PSA PFS, both patients had undetectable serum PSA levels before receiving ipilimumab.

Patient #	# NS mutations	PSA PFS (months)	Radiographic PFS (months)	Best overall response	OS (months)
3	81	0.7	1.7	PD	2.0
10	49	na	2.1	PD	2.6
12	65	3.1	7.3*	SD	8.5
13	2	2.2	3.4	PD	5.3
16	58	na	1.4	PD	5.7
19	49	0.6	3.0	PD	4.2
22	273	0.7	0.7	na	0.7
24	39	0.7	2.9	PD	10.3
25	47	0.7	3.0	PD	5.8
27	41	0.7	2.5	PD	3.4

*The patient's clinical PFS was 5.1 months.

were designated as the "unfavorable" cohort (n = 10) for the correlative studies. The clinical outcomes shown in Fig. 2 and the best overall response of the favorable and unfavorable cohorts are described in Tables 1 and 2.

Interferon-γ–responsive gene signature and tumor-infiltrating lymphocytes are associated with favorable responses to ipilimumab

The presence of tumor-infiltrating lymphocytes and interferon-γ (IFN-γ)–responsive gene signatures have been shown to be predictive of responses to ICB (*7*, *8*, *16*, *17*). Therefore, pretreatment tumor tissues were evaluated using RNA sequencing (RNA-seq). Gene set enrichment analysis (GSEA) of the pretreatment tumors revealed that the IFN-γ response pathway signature was higher in patients in the favorable cohort compared to the unfavorable cohort (Fig. 3A and Table 3). In addition, the favorable cohort had higher T cell gene signatures, including those of cytotoxic and memory T cells (Fig. 3B). These data were further supported by immunohistochemistry (IHC) staining for markers of T cells (e.g., CD3 and CD8), cytotoxicity (e.g., granzyme B), and T cell activation [e.g., programmed cell death–1 (PD-1)] (Fig. 3C). Although intratumoral CD8 density did not correlate with PD ligand 1 (PD-L1) expression on the tumor cells (Fig. 3C, fig. S1A, and Table 3), PD-L1 expression was detectable on the immune cells within the tumor microenvironment in both patient cohorts (Fig. 3C, fig. S1B, and Table 3). Our results suggest that intratumoral CD8 T cell density and an IFN-γ response gene signature may be predictive of responses to ipilimumab and/or prognostic of OS.

Detection of T cell responses to prostate tumor-associated antigens and neoantigens

Somatic mutations may represent cancer neoantigens capable of being recognized by T cells (*6*, *18*–*21*). Consistent with this, neoantigen frequency has been associated with responsiveness to ICB in patients with melanoma treated with ipilimumab (*2*, *3*). To identify potential prostate cancer neoantigens that could be correlated with clinical responses to ipilimumab, whole-exome sequencing (WES) of pretreatment tumor tissues and matched peripheral blood mononuclear cells (PBMCs) was used to detect all potential nonsynonymous mutations (fig. S2). The median number of nonsynonymous somatic mutations was 76 in the cohort of 27 patients (table S5), which was much lower compared to melanoma and NSCLC (median number of nonsynonymous somatic mutations about 200) (*3*, *22*), but was consistent for prostate cancer (*1*, *23*). There was no difference in the TMB from samples obtained from primary versus metastatic sites (fig. S3), and there was no difference in predicted neoantigen frequency (as determined by the in silico prediction algorithm NetMHCpan) between the primary and metastatic sites (fig. S4). Furthermore, TMB was not associated with improved clinical responses to ipilimumab because the median frequency of nonsynonymous mutations was similar between the favorable and unfavorable cohorts (fig. S5).

Next, RNA-seq of the pretreatment tumor tissues was used to identify which of these nonsynonymous mutations were expressed. The expressed mutations were used to develop 23-mer peptides that flanked the mutated amino acids. These peptides were applied to an ex vivo IFN-γ enzyme-linked immunospot (ELISpot) assay with PBMCs to determine which of the expressed mutations elicited T cell responses and thus represented cancer neoantigens. A similar ELISpot assay was used to identify T cell responses to conventional prostate tumor–associated antigens [e.g., prostate-specific membrane antigen (PSMA) and prostatic acid phosphatase (PAP)].

There were sufficient PBMCs to evaluate T cell responses to tumor-associated antigens and neoantigens in 17 of 27 (63%) patients, which accounted for 8 of the 9 patients in the favorable cohort and 4 of the 10 patients in the unfavorable cohort. T cell responses to

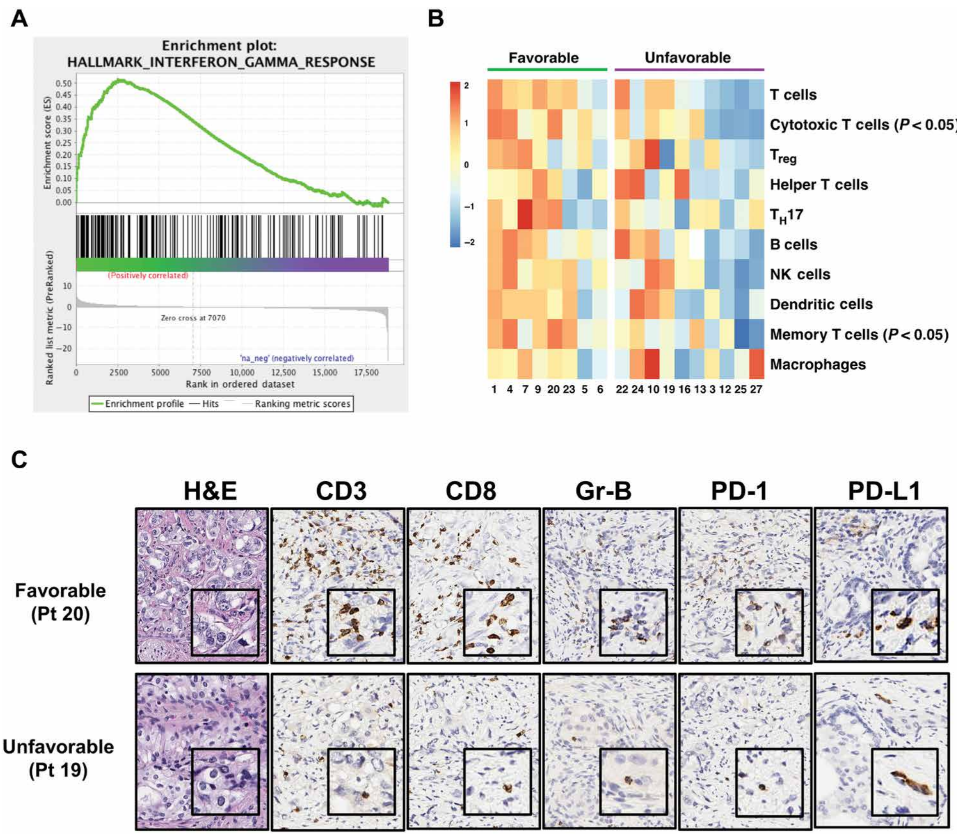

Fig. 3. Immune correlatives in pretreatment tissue associated with the favorable versus the unfavorable cohorts. (**A**) IFN-γ response pathway expression signature in the pretreatment prostate tumor tissues obtained from the favorable cohort (n = 8) versus the unfavorable cohort (n = 10) based on GSEA. (**B**) Intratumoral immune subpopulations in the favorable cohort (n = 8) versus the unfavorable cohort (n = 10) based on RNA-seq analyses. Unpaired t test was used to determine statistical significance. (**C**) T cell infiltration in the favorable cohort versus the unfavorable cohort based on representative IHC staining in pretreatment tissues. A 20× magnification for the large outer squares and a 40× magnification for the small inner squares were used. T_{reg}, regulatory T cell; T_H17, T helper 17 cell; Gr-B, granzyme B.

Table 3. Summary of immune correlatives associated with favorable and unfavorable clinical outcomes. na, not available because of insufficient amount of PBMCs.

		Pretreatment						Posttreatment	
	Patient #	# NS mutations	Genetic deficiency	CD8 density (cells/mm^2)	PD-L1 density (immune cells/mm^2)	PD-L1 % on tumor cells	IFN-γ high (RNA-seq)	PSMA/PAP ELISpot	Neoantigen ELISpot
Favorable	1	41	No	3063	393	0	Yes	Negative	Negative
	4	708	*PSM2*	393	14	0	Yes	Negative	Negative
	5	24	No	282	128	0	No	Negative	Positive
	6	2	No	655	na	na	No	na	na
	7	13	No	606	52	0	No	Positive	Positive
	9	25	No	290	na	na	Yes	Positive	Negative
	15	104	*FANCA*	458	123	0	na	Positive	Negative
	20	31	No	454	86	0	Yes	Negative	Negative
	23	25	No	275	24	0	Yes	Negative	Negative
Unfavorable	3	81	No	197	137	0	No	Negative	Negative
	10	49	No	43	4	0	No	na	na
	12	65	No	118	186	0	No	Negative	Negative
	13	2	No	331	96	0	No	Negative	Negative
	16	58	No	387	1242	0	Yes	na	na
	19	49	No	362	71	0	No	na	na
	22	273	*BRCA2*	136	172	0	Yes	na	na
	24	39	No	42	113	14	No	Negative	Negative
	25	47	No	83	na	na	No	na	na
	27	49	No	na	na	na	No	na	na

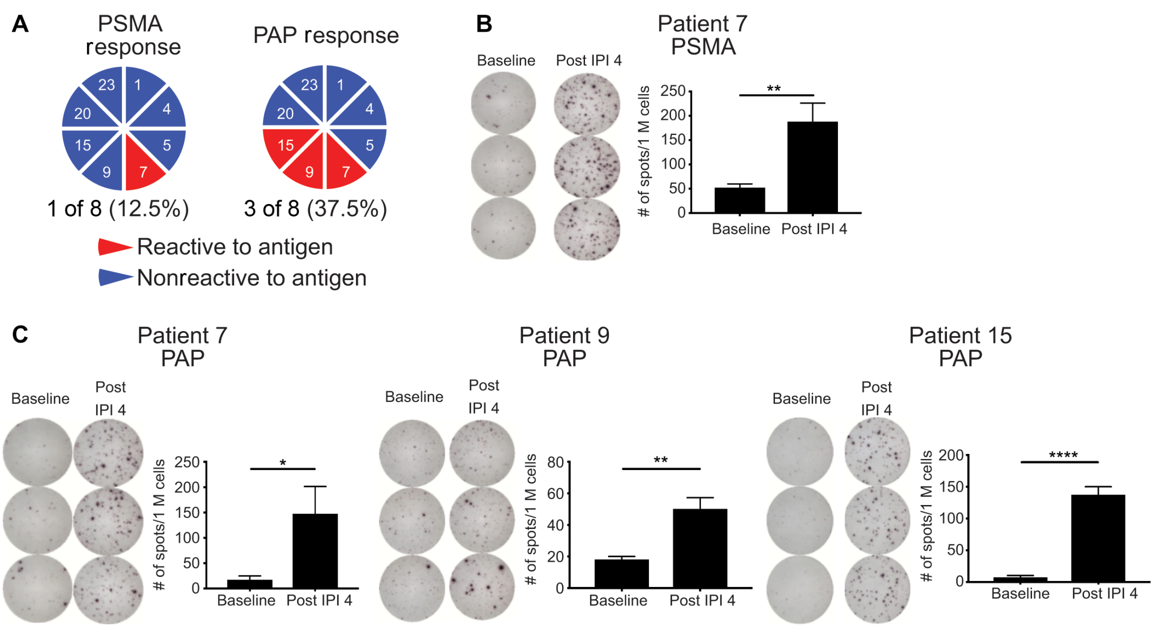

Fig. 4. T cell responses to prostate tumor–associated antigens. (**A**) Pie charts denoting the patients within the favorable cohort with T cell responses against prostate-specific membrane antigen (PSMA) and prostatic acid phosphatase (PAP). (**B**) Raw ELISpot data and graphical representation of T cell responses against PSMA in patient #7. Unpaired *t* test was used to determine statistical significance. $^{**}P \leq 0.01$. (**C**) Raw ELISpot data and graphical representation of T cell responses against PAP in patients #7, #9, and #15. Unpaired *t* test was used to determine statistical significance. $^{*}P \leq 0.05$, $^{**}P \leq 0.01$, and $^{****}P \leq 0.0001$.

PSMA, PAP, and cancer neoantigens were only identified in patients within the favorable cohort (Fig. 4, A to C, and Table 3). Specifically, using this approach for mutant neoantigen detection, T cell responses against somatic mutations in *PCMTD2* (protein-L-isoaspartate *O*-methyltransferase domain–containing protein 2 isoform 1; p. V282A) for patient #5 and *ARHGEF37* (rho guanine nucleotide exchange factor 37; p.R664W) and *DPYS* (dihydropyrimidinase; p.V364M) for patient #7 were identified (Fig. 5, A and B). T cell responses to all three of these cancer neoantigens were undetectable in pretreatment PBMCs but were enhanced after treatment with ipilimumab. Furthermore, all three neoantigens were likely major histocompatibility complex (MHC) class I restricted because depletion of CD8 T cells, but not CD4 T cells, resulted in attenuation of T cell–mediated IFN-γ responses in ELISpot assays (Fig. 5, A and B). Clustering analyses confirmed that all three of the identified neoantigens were clonal, and they were present in all tumor cells. These neoantigens also were predicted by NetMHCpan (table S6).

Prostate cancers harboring mutations in mismatch repair (MMR) and DNA damage repair (DDR) genes or those with biallelic cyclin-dependent kinase 12 loss have high TMB and have been associated with increased responses to ICB (*19*, *24*, *25*). However, two of the patients in the favorable cohort and one patient in the unfavorable cohort had tumors with somatic missense mutations in an MMR gene, *PSM2* (patient #4), and DDR genes, *FANCA* (patient #15) and

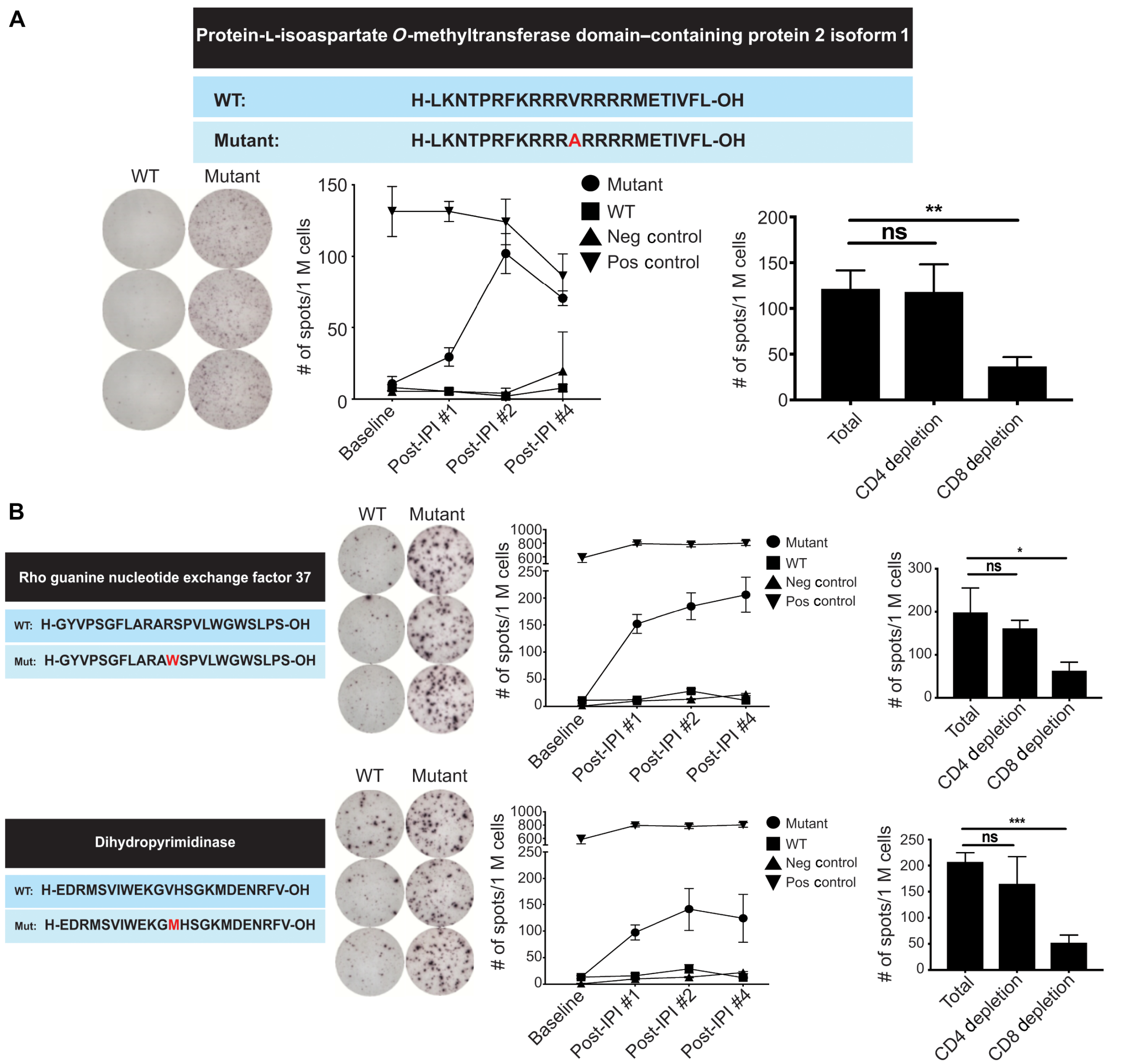

Fig. 5. T cell responses to prostate cancer neoantigens. (**A**) T cell responses against protein-L-isoaspartate *O*-methyltransferase domain–containing protein 2 isoform 1 in patient #5 before and after ipilimumab treatment. The table (top) demonstrates the amino acid change between the wild-type (WT) and mutant sequences. Raw ELISpot data (bottom left) and graphical representation of T cell responses (bottom middle) against the neoantigen are shown. Depletion of CD4 or CD8 T cells in ELISpot assays (bottom right) against the neoantigens is shown. Unpaired *t* test was used to determine statistical significance. $^{**}P \leq 0.01$. ns, not significant. (**B**) T cell responses against rho guanine nucleotide exchange factor 37 and dihydropyrimidinase in patient #7 before and after ipilimumab treatment. The tables (left) demonstrate the amino acid changes between the wild-type and mutant sequences. Raw ELISpot data (left middle) and graphical representation of T cell responses (right middle) against the neoantigens are shown. Depletion of CD4 or CD8 T cells in ELISpot assays (right) against the neoantigens is shown. Unpaired *t* test was used to determine statistical significance. $^{*}P \leq 0.05$ and $^{***}P \leq 0.001$.

BRCA2 (patient #22), which were associated with a relatively high TMB (>76, median number nonsynonymous mutations). Unexpectedly, for these three patients, there were no detectable T cell–mediated IFN-γ responses to cancer neoantigens (Table 3), which may be attributed to lack of detection by the ELISpot assay or inability to identify neoantigens that occur as a result of splice variants or indels, as opposed to single-nucleotide variants (SNVs).

DISCUSSION

Unlike melanoma or NSCLC (2-5), our data suggest that high TMB was not required for neoantigen detection, or for the selection of patients with mCRPC who were likely to benefit from ICB. Pretreatment tumor tissues from patients in the favorable cohort had relatively low TMB, but they were found to have (i) intratumoral CD8 density greater than 400 cells/mm^2, (ii) high IFN-γ response gene signature, (iii) antigen-specific T cell responses, or (iv) a combination of these immune correlatives. Six of nine (67%) patients in the favorable cohort currently are alive; whereas all 10 patients in the unfavorable cohort have succumbed to their disease. The hypothesis that the immunological correlatives listed above may reliably identify mCRPC patients who benefit from ICB will need to be tested in a much larger patient cohort.

We have shown that anti–CTLA-4 therapy significantly enhanced tumor-specific T cell responses in patients with mCRPC who have relatively low TMB because the frequency of nonsynonymous mutations for patients #5 and #7 were 24 and 13, respectively. Note that we relied on an undirected approach to identify prostate cancer neoantigens. This strategy was optimized to detect neoantigens derived from SNVs, and there was a possibility that the frequency of neoantigens derived from insertion and deletion mutations (indels) was underestimated. Nevertheless, we confirmed that these neoantigens would have been predicted by the NetMHCpan algorithm, which provides credibility for using this in silico approach to rapidly predict neoantigens for vaccine clinical trials. Moreover, on the basis of recent reports of neoantigen vaccines being developed for patients with melanoma and glioblastoma multiforme (*20*, *26*), we propose that prostate cancer represents another tumor type where neoantigen vaccines can be considered, especially in combination strategies with ICB, as a potential therapy to improve clinical outcomes. There are ongoing clinical trials evaluating vaccines plus ICB (ClinicalTrials.gov) in prostate cancer and other malignancies, and the results are pending.

These data with ipilimumab in our small cohort of patients are comparable to the data with pembrolizumab monotherapy in treatment-refractory mCRPC, which reported a median radiographic PFS of 2.1 months, median OS of 9.6 months, and a DCR of 20% (*27*). As our clinical trial was completing accrual, we found that clinical responses to ipilimumab were attenuated, at least in part, by adaptive resistance due to up-regulation of the immune checkpoints, PD-L1 and V-domain Ig Suppressor of T cell Activation (VISTA), within the prostate tumor microenvironment (*28*). In our current study, there were no significant radiographic responses observed in patients treated with ipilimumab monotherapy; however, the combination of nivolumab (anti–PD-1) plus ipilimumab in men with mCRPC (CheckMate 650; NCT02985957) induced significant antitumor responses including partial and complete regression of disease in a subset of patients (*23*). Furthermore, both CheckMate 650 and our current study identified similar median TMB values (74.5 and 76 nonsynonymous mutations, respectively) for mCRPC, which were considerably lower than the median TMB observed in melanoma and NSCLC (~200 nonsynonymous mutations) (*3*, *22*). Despite the relatively low TMB and few mutations identified in mCRPC, our study demonstrates that some of these mutations are capable of inducing antigen-specific T cell responses.

Together, our results suggest that a particular subset of patients may benefit from ICB, despite having a relatively low TMB. Moreover, they also suggest that pretreatment tissue correlatives such as CD8 T cells and IFN-γ response gene signature may improve patient selection for treatment with ICB, particularly for those cancers with low TMB. In summary, our clinical study provides data to support further testing of immunotherapy strategies in patients with metastatic prostate cancer.

MATERIALS AND METHODS

Study design

Thirty men with mCRPC were enrolled to a feasibility clinical study (NCT02113657; MD Anderson protocol 2013-0444) to determine T cell responses to neoantigens after treatment with ipilimumab. The trial objectives were to obtain preliminary estimates of the impact of ipilimumab on T cell responses to neoantigens, other immunological variables, and clinical outcomes (e.g., PSA kinetics, radiographic responses, and drug-related toxicities) in patients with mCRPC. The sample size ensured that the trial was not terminated early because of toxicity. Safety monitoring rules were in place to stop the study if the probability of toxicity was greater than 25%. To be eligible, patients had to be at least 18 years of age and have histologically confirmed prostate carcinoma, with radiographic evidence of metastatic disease. Patients also had to demonstrate tumor progression while on hormone therapy with castrate serum testosterone (≤1.7 nM or 50 ng/dl) with biopsy-proven viable disease, PSA, and/or radiographic progression according to the Prostate Cancer Clinical Trials Working Group 2 (*29*). Furthermore, patients must have had a resected prostate cancer mass (primary and/or metastatic site) within 3 months of study entry. Other eligibility criteria included adequate hematological, renal, and hepatic function and an Eastern Cooperative Oncology Group performance status of 0 to 1. The clinical trial was approved by the institutional review board at The University of Texas MD Anderson Cancer Center. Written informed consent for participation in the study was obtained from all participants. In addition, all patients provided informed consent on The University of Texas MD Anderson Cancer Center institutional-approved laboratory protocol (PA13-0291) for tissue and blood collection for the study. Primary data are reported in data file S1.

Isolation of mononuclear cells from peripheral blood

Mononuclear cells were isolated from patients by Ficoll-Paque density gradient centrifugation and cryopreserved. The frozen cells were rapidly thawed by immersion in a 37°C water bath with gentle agitation. Cells were washed and incubated at 37°C for 20 min in 10 ml of Dulbecco's modified Eagle medium (DMEM; Corning) containing deoxyribonuclease (STEMCELL Technologies). The mononuclear cells were washed using Iscove's modified DMEM supplemented with human AB serum (5%), 2-mercaptoethanol (50 μM), gentamicin (20 μg/ml), penicillin (1000 IU/ml), streptomycin (100 μg/ml), and Hepes (Sigma-Aldrich). Cell counts and viability were determined using Nexcelom Counting Chamber and acridine orange/propidium iodide staining solution (Nexcelom Bioscience).

WES and transcriptome analyses for neoantigen identification
Total RNA and DNA were extracted from the tumor tissues and PBMCs using either Qiagen DNA mini kit or Qiagen formalin-fixed paraffin-embedded (FFPE) DNA kit as per the manufacturer's instructions. RNA was extracted using either an RNEasy Mini kit (Qiagen) or an RNA FFPE kit (Qiagen). Library preparation, DNA sequencing, and RNA-seq were performed at The University of Texas MD Anderson Cancer Center Cancer Genomics Laboratory. For WES, genomic DNA (250 ng) was sheared using Covaris S2 focused ultrasonicator (Covaris), using the standard protocol for a final library insert size of 150 to 200 base pairs (bp). KAPA Hyper-Prep kit with Agilent SureSelect Human All Exon v4 was used for end repair, A-base addition, adaptor ligation, and library enrichment polymerase chain reaction (PCR). The hybridization reaction was then performed as per the manufacturer's instructions using the SureSelect Target Enrichment Protocol. The libraries were normalized to equal concentrations using a QuantStudio 6 Flex (Applied Bio-systems) instrument and the KAPA library quantification kit. DNA libraries were quantified through quantitative PCR using the Agilent TapeStation. Sequencing was done on the HiSeq 2500 platform (76 bp paired end) at about 200× coverage for tumor samples and 100× for normal samples. For RNA-seq, RNA quality control was performed using the Agilent Bioanalyzer. cDNA preparation and Illumina sequencing libraries were constructed from total RNA using the NuGEN Ovation RNA-Seq FFPE and Ultralow System v2 library preparation system as per the manufacturer's protocol. The libraries were sequenced on the Illumina HiSeq system with 76-bp paired-end reads. BCL files were processed using Illumina's Consensus Assessment of Sequence and Variation tool (https://www.illumina.com/documents/products/datasheets/datasheet_genomic_sequence.pdf) for demultiplexing/conversion to FASTQ format. The DNA FASTQ files were aligned to the reference genome (human Hg19; University of California, Santa Cruz genome browser: genome.ucsc.edu) using the burrows-wheeler aligner (BWA) with three mismatches with two in the first 40 seed regions (*30*). RNA FASTQ files were processed using STAR after the two-step alignment procedure (*31*). The aligned compressed binary version of sequence alignment map (BAM) files were subjected to mark duplication, realignment, and recalibration using Picard and genome analysis toolkit (GATK) before any downstream analyses (*32*). Mutations were called using MuTect for DNA and Platypus for RNA. Nonsynonymous mutations detected by MuTect and confirmed to be expressed in RNA mutation calls were used as input to NetMHCpan (http://www.cbs.dtu.dk/services/NetMHCpan/) for neoantigen prediction. The smallest number of the binding nanomolar values from all possible 8- to 12-mer peptides containing the mutated amino acid of interest was defined as the predicted MHC binding score. For prediction of putative neoantigens, the following two filters were applied in sequence: (i) RNA transcripts per million >1 and (ii) binding affinity <500 nM.

IFN-γ ELISpot assay
IFN-γ ELISpot assay for 17 patients was performed using Millipore MultiScreen-HA 96-well filter plates (Millipore). Plates were coated with anti–IFN-γ (5 μg/ml) monoclonal antibody (mAb; clone 1-D1K, Mabtech) in pH 9.5 carbonate buffer (Sigma-Aldrich) overnight at 4°C and blocked with phosphate-buffered saline (PBS) and 2% bovine serum albumin (Sigma-Aldrich). The PBMCs (500,000 cells per well), peptides, and the control peptides (10 μM) were added to the plates and incubated for 16 hours at 37°C. Cells were washed away, and plates were incubated with biotin-labeled anti–IFN-γ mAb (clone 7-B6-1, Mabtech) for 1 hour at room temperature. Plates were washed with 1× PBS (Sigma-Aldrich). The plates were incubated with extravidin-alkaline phosphatase (1:5000; Sigma-Aldrich) for 1.5 hours at room temperature. Plates were developed with filtered 5-bromo-4-chloro-3-indolyl-phosphate in conjunction with nitro blue tetrazolium (Sigma-Aldrich). Spots were counted on an ImmunoSpot ELISpot reader (CTL Immunospot Reader, software version 5.1.36). Cells treated with phorbol 12-myristate 13-acetate (Sigma-Aldrich) and ionomycin (Sigma-Aldrich) were used as positive controls in all experiments. Peptide recognition was considered positive when the spots were two times higher than the negative control (HIV-gag peptide, RS Synthesis). Wild-type peptides (PepMix pool, JPT Peptide Technologies) from proteins tested used in this study were used at a concentration of 10 μM: PSMA 185 peptides 15-mers with 11–amino acid overlap and PAP 94 peptides 15-mers with 11–amino acid overlap. Patient-specific wild-type and mutant peptides were bought from either JPT Peptide Technologies or GenScript. Each peptide was a 23-mer with mutant amino acid in the middle flanked by 11-mers on each side.

Immunohistochemistry
IHC was performed on FFPE tumor tissue. Tumor tissues were fixed in 10% formalin, embedded in paraffin, and transversely sliced into 4-μm sections. Sections were then stained with hematoxylin and eosin (H&E), and consecutive serial sections were stained for IHC using mouse anti-human mAbs against CD3 (Dako, catalog no.A0452), CD8 (Thermo Scientific, MS-457-S), granzyme B (Leica Microsystems, PA0291), PD-1 (Abcam, ab137132), and PD-L1 (Cell Signaling Technology, 13684S). Sections were processed with peroxidase-conjugated avidin/biotin and 3′-3-diaminobenzidine substrate (Leica Microsystem), and the IHC slides were scanned and digitalized using the ScanScope XT system (Aperio/Leica Technologies). IHC staining for each marker was analyzed in conjunction with H&E-stained sections, which facilitated the identification of malignant cells and thus directed IHC quantification. Quantification analysis was performed by the pathologist using the HALO software (Indica Labs, region analysis and quantification modules). The number of positive cells was calculated for each area at 20× magnification, and the retrieved data are expressed as density (absolute number of positive cells per square millimeter).

Immune profiling of tumor microenvironment
Markers for 10 immune cell types, including T cell, cytotoxic T cell, regulatory T cell, helper T cell, T helper 17 cell, B cell, natural killer cell, dendritic cell, memory T cell, and macrophage, were obtained from the PanCancer Immune Profiling Panel developed by NanoString Technologies Inc. RNA-seq raw read counts were transformed to log2 scale by variance stabilizing transformation. The variation of activity of each immune cell type across samples was estimated by gene set variation analysis (*33*).

Gene set enrichment analysis
GSEA was performed to identify pathways differentially expressed between responders and nonresponders. RNA-seq raw counts were normalized by Bioconductor Package DESeq2 (*34*). The *P* value and $\log_2$ fold change (FC) of each gene were generated by differential expression analysis in DESeq2. The rank score of gene was calculated as $\text{rnk} = I(\text{ sign }) * (-1) * \log_{10}(P)$, where $I(\text{ sign })$ is an indicator variable that is 1 if $\log_2(\text{FC}) \geq 0$ but otherwise is −1. GSEA was carried out using the GSEAPreranked module with default parameters based on gene

rank scores (*35*). Hallmark gene sets from the Molecular Signature Database (http://software.broadinstitute.org/gsea/msigdb) were used for pathway analysis, and pathways with less than 15 genes or more than 500 genes were filtered to avoid overly narrow or broad functional categories. In this study, we set the false discovery rate (FDR) cutoff to 0.01, namely, pathways with FDR <0.01 were considered to be significantly differentially expressed.

Time to event estimates

Median PFS, OS, and follow-up time distributions from the date of treatment initiation with ipilimumab were estimated by the Kaplan-Meier method. PSA PFS (death without progression is an event) was measured from the date of treatment start until defined PSA progression. Patients who started with PSA equal to 0 ng/ml were excluded from PSA progression assessment. Patients who received abiraterone acetate before developing PSA progression were censored on that date. Radiographic and clinical PFS were similarly measured from treatment start until progression noted by that modality (death without progression is an event). Kaplan-Meier estimates were calculated in SAS 9.4 (SAS Institute) and curves were created in Stata 14.2 (StataCorp LLC).

Statistical analyses

Statistical analyses were performed using Prism version 8 (GraphPad), with selection of the test as outlined in the results and figure legends. *P* values of ≤0.05 were considered statistically significant.

SUPPLEMENTARY MATERIALS

stm.sciencemag.org/cgi/content/full/12/537/eaaz3577/DC1
Fig. S1. Representative PD-L1 IHC staining within the prostate tumor microenvironment.
Fig. S2. Schema on identifying tumor-specific mutations and T cell responses to cancer neoantigens.
Fig. S3. Number of nonsynonymous mutations in primary and metastatic prostate cancers.
Fig. S4. Number of predicted neoantigens in primary versus metastatic prostate cancer using NetMHCpan.
Fig. S5. Number of nonsynonymous mutations in the prostate tumor tissues obtained from the favorable versus unfavorable cohorts.
Table S1. Baseline characteristics and laboratory values.
Table S2. Metastatic distribution of the patients at baseline.
Table S3. Prior systemic therapies.
Table S4. Selected irAEs.
Table S5. Identifying potential neoantigens with WES and RNA-seq.
Table S6. Comparison of identified and predicted neoantigens.
Data file S1. Primary data.
Clinical protocol

View/request a protocol for this paper from *Bio-protocol*.

REFERENCES AND NOTES

1. L. B. Alexandrov, S. Nik-Zainal, D. C. Wedge, S. A. J. R. Aparicio, S. Behjati, A. V. Biankin, G. R. Bignell, N. Bolli, A. Borg, A.-L. Børresen-Dale, S. Boyault, B. Burkhardt, A. P. Butler, C. Caldas, H. R. Davies, C. Desmedt, R. Eils, J. E. Eyfjörd, J. A. Foekens, M. Greaves, F. Hosoda, B. Hutter, T. Ilicic, S. Imbeaud, M. Imielinski, N. Jäger, D. T. W. Jones, D. Jones, S. Knappskog, M. Kool, S. R. Lakhani, C. López-Otín, S. Martin, N. C. Munshi, H. Nakamura, P. A. Northcott, M. Pajic, E. Papaemmanuil, A. Paradiso, J. V. Pearson, X. S. Puente, K. Raine, M. Ramakrishna, A. L. Richardson, J. Richter, P. Rosenstiel, M. Schlesner, T. N. Schumacher, P. N. Span, J. W. Teague, Y. Totoki, A. N. J. Tutt, R. Valdés-Mas, M. M. van Buuren, L. van 't Veer, A. Vincent-Salomon, N. Waddell, L. R. Yates; Australian Pancreatic Cancer Genome Initiative; ICGC Breast Cancer Consortium; ICGC MMML-Seq Consortium; ICGC Ped Brain, J. Zucman-Rossi, P. A. Futreal, U. M. Dermott, P. Lichter, M. Meyerson, S. M. Grimmond, R. Siebert, E. Campo, T. Shibata, S. M. Pfister, P. J. Campbell, M. R. Stratton, Signatures of mutational processes in human cancer. *Nature* **500**, 415–421 (2013).
2. A. Snyder, V. Makarov, T. Merghoub, J. Yuan, J. M. Zaretsky, A. Desrichard, L. A. Walsh, M. A. Postow, P. Wong, T. S. Ho, T. J. Hollmann, C. Bruggeman, K. Kannan, Y. Li, C. Elipenahli, C. Liu, C. T. Harbison, L. Wang, A. Ribas, J. D. Wolchok, T. A. Chan, Genetic basis for clinical response to CTLA-4 blockade in melanoma. *N. Engl. J. Med.* **371**, 2189–2199 (2014).
3. E. M. Van Allen, D. Miao, B. Schilling, S. A. Shukla, C. Blank, L. Zimmer, A. Sucker, U. Hillen, M. H. Geukes Foppen, S. M. Goldinger, J. Utikal, J. C. Hassel, B. Weide, K. C. Kaehler, C. Loquai, P. Mohr, R. Gutzmer, R. Dummer, S. Gabriel, C. J. Wu, D. Schadendorf, L. A. Garraway, Genomic correlates of response to CTLA–4 blockade in metastatic melanoma. *Science* **350**, 207–211 (2015).
4. N. McGranahan, A. J. S. Furness, R. Rosenthal, S. Ramskov, R. Lyngaa, S. K. Saini, M. Jamal-Hanjani, G. A. Wilson, N. J. Birkbak, C. T. Hiley, T. B. K. Watkins, S. Shafi, N. Murugaesu, R. Mitter, A. U. Akarca, J. Linares, T. Marafioti, J. Y. Henry, E. M. Van Allen, D. Miao, B. Schilling, D. Schadendorf, L. A. Garraway, V. Makarov, N. A. Rizvi, A. Snyder, M. D. Hellmann, T. Merghoub, J. D. Wolchok, S. A. Shukla, C. J. Wu, K. S. Peggs, T. A. Chan, S. R. Hadrup, S. A. Quezada, C. Swanton, Clonal neoantigens elicit T cell immunoreactivity and sensitivity to immune checkpoint blockade. *Science* **351**, 1463–1469 (2016).
5. M. D. Hellmann, T. Nathanson, H. Rizvi, B. C. Creelan, F. Sanchez-Vega, A. Ahuja, A. Ni, J. B. Novik, L. M. B. Mangarin, M. Abu-Akeel, C. Liu, J. L. Sauter, N. Rekhtman, E. Chang, M. K. Callahan, J. E. Chaft, M. H. Voss, M. Tenet, X.-M. Li, K. Covello, A. Renninger, P. Vitazka, W. J. Geese, H. Borghaei, C. M. Rudin, S. J. Antonia, C. Swanton, J. Hammerbacher, T. Merghoub, N. McGranahan, A. Snyder, J. D. Wolchok, Genomic features of response to combination immunotherapy in patients with advanced non-small-cell lung cancer. *Cancer Cell* **33**, 843–852.e4 (2018).
6. H. Matsushita, M. D. Vesely, D. C. Koboldt, C. G. Rickert, R. Uppaluri, V. J. Magrini, C. D. Arthur, J. M. White, Y.-S. Chen, L. K. Shea, J. Hundal, M. C. Wendl, R. Demeter, T. Wylie, J. P. Allison, M. J. Smyth, L. J. Old, E. R. Mardis, R. D. Schreiber, Cancer exome analysis reveals a T-cell-dependent mechanism of cancer immunoediting. *Nature* **482**, 400–404 (2012).
7. R. S. Herbst, J.-C. Soria, M. Kowanetz, G. D. Fine, O. Hamid, M. S. Gordon, J. A. Sosman, D. F. McDermott, J. D. Powderly, S. N. Gettinger, H. E. Kohrt, L. Horn, D. P. Lawrence, S. Rost, M. Leabman, Y. Xiao, A. Mokatrin, H. Koeppen, P. S. Hegde, I. Mellman, D. S. Chen, F. S. Hodi, Predictive correlates of response to the anti-PD-L1 antibody MPDL3280A in cancer patients. *Nature* **515**, 563–567 (2014).
8. P. C. Tumeh, C. L. Harview, J. H. Yearley, I. P. Shintaku, E. J. M. Taylor, L. Robert, B. Chmielowski, M. Spasic, G. Henry, V. Ciobanu, A. N. West, M. Carmona, C. Kivork, E. Seja, G. Cherry, A. J. Gutierrez, T. R. Grogan, C. Mateus, G. Tomasic, J. A. Glaspy, R. O. Emerson, H. Robins, R. H. Pierce, D. A. Elashoff, C. Robert, A. Ribas, PD-1 blockade induces responses by inhibiting adaptive immune resistance. *Nature* **515**, 568–571 (2014).
9. T. M. Beer, E. D. Kwon, C. G. Drake, K. Fizazi, C. Logothetis, G. Gravis, V. Ganju, J. Polikoff, F. Saad, P. Humanski, J. M. Piulats, P. G. Mella, S. S. Ng, D. Jaeger, F. X. Parnis, F. A. Franke, J. Puente, R. Carvajal, L. Sengeløv, M. B. McHenry, A. Varma, A. J. van den Eertwegh, W. Gerritsen, Randomized, double-blind, phase III trial of ipilimumab versus placebo in asymptomatic or minimally symptomatic patients with metastatic chemotherapy-naive castration-resistant prostate cancer. *J. Clin. Oncol.* **35**, 40–47 (2017).
10. E. D. Kwon, C. G. Drake, H. I. Scher, K. Fizazi, A. Bossi, A. J. van den Eertwegh, M. Krainer, N. Houede, R. Santos, H. Mahammedi, S. Ng, M. Maio, F. A. Franke, S. Sundar, N. Agarwal, A. M. Bergman, T. E. Ciuleanu, E. Korbenfeld, L. Sengeløv, S. Hansen, C. Logothetis, T. M. Beer, M. B. McHenry, P. Gagnier, D. Liu, W. R. Gerritsen; CA184-043 Investigators, Ipilimumab versus placebo after radiotherapy in patients with metastatic castration-resistant prostate cancer that had progressed after docetaxel chemotherapy (CA184-043): A multicentre, randomised, double-blind, phase 3 trial. *Lancet Oncol.* **15**, 700–712 (2014).
11. S. K. Subudhi, A. Aparicio, J. Gao, A. J. Zurita, J. C. Araujo, C. J. Logothetis, S. A. Tahir, B. R. Korivi, R. S. Slack, L. Vence, R. O. Emerson, E. Yusko, M. Vignali, H. S. Robins, J. Sun, J. P. Allison, P. Sharma, Clonal expansion of CD8 T cells in the systemic circulation precedes development of ipilimumab-induced toxicities. *Proc. Natl. Acad. Sci. U.S.A.* **113**, 11919–11924 (2016).
12. E. J. Small, N. Tchekmedyian, B. I. Rini, L. Fong, I. Lowy, J. P. Allison, A pilot trial of CTLA-4 blockade with human anti-CTLA-4 in patients with hormone-refractory prostate cancer. *Clin. Cancer Res.* **13**, 1810–1815 (2007).
13. T. Beer, S. Slovin, C. Higano, S. Tejwani, T. Dorff, E. Stankevich, I. Lowy, Phase I trial of ipilimumab (IPI) alone and in combination with radiotherapy (XRT) in patients with metastatic castration resistant prostate cancer (mCRPC). *J. Clin. Oncol.* **26**, 5004–5004 (2008).
14. W. Gerritsen, A. van den Eertwegh, T. de Gruijl, H. van den Berg, R. Scheper, N. Sacks, I. Lowy, E. Stankevich, K. Hege, Expanded phase I combination trial of GVAX immunotherapy for prostate cancer and ipilimumab in patients with metastatic hormone-refractory prostate cancer (mHPRC). *J. Clin. Oncol.* **26**, 5146–5146 (2008).
15. J. Gao, Q. He, S. Subudhi, A. Aparicio, A. Zurita-Saavedra, D. H. Lee, C. Jimenez, M. Suarez-Almazor, P. Sharma, Review of immune-related adverse events in prostate cancer patients treated with ipilimumab: MD Anderson experience. *Oncogene* **34**, 5411–5417 (2015).

16. O. Hamid, H. Schmidt, A. Nissan, L. Ridolfi, S. Aamdal, J. Hansson, M. Guida, D. M. Hyams, H. Gómez, L. Bastholt, S. D. Chasalow, D. Berman, A prospective phase II trial exploring the association between tumor microenvironment biomarkers and clinical activity of ipilimumab in advanced melanoma. *J. Transl. Med.* **9**, 204 (2011).
17. M. Ayers, J. Lunceford, M. Nebozhyn, E. Murphy, A. Loboda, D. R. Kaufman, A. Albright, J. D. Cheng, S. P. Kang, V. Shankaran, S. A. Piha-Paul, J. Yearley, T. Y. Seiwert, A. Ribas, T. K. McClanahan, IFN-γ-related mRNA profile predicts clinical response to PD-1 blockade. *J. Clin. Invest.* **127**, 2930–2940 (2017).
18. N. H. Segal, D. W. Parsons, K. Peggs, V. Velculescu, K. W. Kinzler, B. Vogelstein, J. P. Allison, Epitope landscape in breast and colorectal cancer. *Cancer Res.* **68**, 889–892 (2008).
19. T. N. Schumacher, R. D. Schreiber, Neoantigens in cancer immunotherapy. *Science* **348**, 69–74 (2015).
20. P. A. Ott, Z. Hu, D. B. Keskin, S. A. Shukla, J. Sun, D. J. Bozym, W. Zhang, A. Luoma, A. Giobbie-Hurder, L. Peter, C. Chen, O. Olive, T. A. Carter, S. Li, D. J. Lieb, T. Eisenhaure, E. Gjini, J. Stevens, W. J. Lane, I. Javeri, K. Nellaiappan, A. M. Salazar, H. Daley, M. Seaman, E. I. Buchbinder, C. H. Yoon, M. Harden, N. Lennon, S. Gabriel, S. J. Rodig, D. H. Barouch, J. C. Aster, G. Getz, K. Wucherpfennig, D. Neuberg, J. Ritz, E. S. Lander, E. F. Fritsch, N. Hacohen, C. J. Wu, An immunogenic personal neoantigen vaccine for patients with melanoma. *Nature* **547**, 217–221 (2017).
21. M. M. Gubin, X. Zhang, H. Schuster, E. Caron, J. P. Ward, T. Noguchi, Y. Ivanova, J. Hundal, C. D. Arthur, W.-J. Krebber, G. E. Mulder, M. Toebes, M. D. Vesely, S. S. K. Lam, A. J. Korman, J. P. Allison, G. J. Freeman, A. H. Sharpe, E. L. Pearce, T. N. Schumacher, R. Aebersold, H.-G. Rammensee, C. J. M. Melief, E. R. Mardis, W. E. Gillanders, M. N. Artyomov, R. D. Schreiber, Checkpoint blockade cancer immunotherapy targets tumour-specific mutant antigens. *Nature* **515**, 577–581 (2014).
22. N. A. Rizvi, M. D. Hellmann, A. Snyder, P. Kvistborg, V. Makarov, J. J. Havel, W. Lee, J. Yuan, P. Wong, T. S. Ho, M. L. Miller, N. Rekhtman, A. L. Moreira, F. Ibrahim, C. Bruggeman, B. Gasmi, R. Zappasodi, Y. Maeda, C. Sander, E. B. Garon, T. Merghoub, J. D. Wolchok, T. N. Schumacher, T. A. Chan, Mutational landscape determines sensitivity to PD-1 blockade in non–small cell lung cancer. *Science* **348**, 124–128 (2015).
23. P. Sharma, R. K. Pachynski, V. Narayan, A. Flechon, G. Gravis, M. D. Galsky, H. Mahammedi, A. Patnaik, S. K. Subudhi, M. Ciprotti, T. Duan, A. Saci, S. Hu, G. C. Han, K. Fizazi, Initial results from a phase II study of nivolumab (NIVO) plus ipilimumab (IPI) for the treatment of metastatic castration-resistant prostate cancer (mCRPC; CheckMate 650). *J. Clin. Oncol.* **37**, 142 (2019).
24. D. T. Le, J. N. Durham, K. N. Smith, H. Wang, B. R. Bartlett, L. K. Aulakh, S. Lu, H. Kemberling, C. Wilt, B. S. Luber, F. Wong, N. S. Azad, A. A. Rucki, D. Laheru, R. Donehower, A. Zaheer, G. A. Fisher, T. S. Crocenzi, J. J. Lee, T. F. Greten, A. G. Duffy, K. K. Ciombor, A. D. Eyring, B. H. Lam, A. Joe, S. P. Kang, M. Holdhoff, L. Danilova, L. Cope, C. Meyer, S. Zhou, R. M. Goldberg, D. K. Armstrong, K. M. Bever, A. N. Fader, J. Taube, F. Housseau, D. Spetzler, N. Xiao, D. M. Pardoll, N. Papadopoulos, K. W. Kinzler, J. R. Eshleman, B. Vogelstein, R. A. Anders, L. A. Diaz Jr., Mismatch repair deficiency predicts response of solid tumors to PD-1 blockade. *Science* **357**, 409–413 (2017).
25. Y.-M. Wu, M. Cieslik, R. J. Lonigro, P. Vats, M. A. Reimers, X. Cao, Y. Ning, L. Wang, L. P. Kunju, N. de Sarkar, E. I. Heath, J. Chou, F. Y. Feng, P. S. Nelson, J. S. de Bono, W. Zou, B. Montgomery, A. Alva; PCF/SU2C International Prostate Cancer Dream Team, D. R. Robinson, A. M. Chinnaiyan, Inactivation of *CDK12* delineates a distinct immunogenic class of advanced prostate cancer. *Cell* **173**, 1770–1782.e14 (2018).
26. D. B. Keskin, A. J. Anandappa, J. Sun, I. Tirosh, N. D. Mathewson, S. Li, G. Oliveira, A. Giobbie-Hurder, K. Felt, E. Gjini, S. A. Shukla, Z. Hu, L. Li, P. M. Le, R. L. Allesøe, A. R. Richman, M. S. Kowalczyk, S. Abdelrahman, J. E. Geduldig, S. Charbonneau, K. Pelton, J. B. Iorgulescu, L. Elagina, W. Zhang, O. Olive, C. McCluskey, L. R. Olsen, J. Stevens, W. J. Lane, A. M. Salazar, H. Daley, P. Y. Wen, E. A. Chiocca, M. Harden, N. J. Lennon, S. Gabriel, G. Getz, E. S. Lander, A. Regev, J. Ritz, D. Neuberg, S. J. Rodig, K. L. Ligon, M. L. Suva, K. W. Wucherpfennig, N. Hacohen, E. F. Fritsch, K. J. Livak, P. A. Ott, C. J. Wu, D. A. Reardon, Neoantigen vaccine generates intratumoral T cell responses in phase Ib glioblastoma trial. *Nature* **565**, 234–239 (2019).
27. E. S. Antonarakis, J. M. Piulats, M. Gross-Goupil, J. Goh, K. Ojamaa, C. J. Hoimes, U. Vaishampayan, R. Berger, A. Sezer, T. Alanko, R. de Wit, C. Li, A. Omlin, G. Procopio, S. Fukasawa, K.-i. Tabata, S. H. Park, S. Feyerabend, C. G. Drake, H. Wu, P. Qiu, J. Kim, C. Poehlein, J. S. de Bono, Pembrolizumab for treatment-refractory metastatic castration-resistant prostate cancer: Multicohort, open-label phase II KEYNOTE-199 study. *J. Clin. Oncol.* **38**, 395–405 (2019).
28. J. Gao, J. F. Ward, C. A. Pettaway, L. Z. Shi, S. K. Subudhi, L. M. Vence, H. Zhao, J. Chen, H. Chen, E. Efstathiou, P. Troncoso, J. P. Allison, C. J. Logothetis, I. I. Wistuba, M. A. Sepulveda, J. Sun, J. Wargo, J. Blando, P. Sharma, VISTA is an inhibitory immune checkpoint that is increased after ipilimumab therapy in patients with prostate cancer. *Nat. Med.* **23**, 551–555 (2017).
29. H. I. Scher, M. J. Morris, W. M. Stadler, C. Higano, E. Basch, K. Fizazi, E. S. Antonarakis, T. M. Beer, M. A. Carducci, K. N. Chi, P. G. Corn, J. S. de Bono, R. Dreicer, D. J. George, E. I. Heath, M. Hussain, W. K. Kelly, G. Liu, C. Logothetis, D. Nanus, M. N. Stein, D. E. Rathkopf, S. F. Slovin, C. J. Ryan, O. Sartor, E. J. Small, M. R. Smith, C. N. Sternberg, M.-E. Taplin, G. Wilding, P. S. Nelson, L. H. Schwartz, S. Halabi, P. W. Kantoff, A. J. Armstrong; Prostate Cancer Clinical Trials Working, Trial design and objectives for castration-resistant prostate cancer: Updated recommendations from the Prostate Cancer Clinical Trials Working Group 3. *J. Clin. Oncol.* **34**, 1402–1418 (2016).
30. H. Li, R. Durbin, Fast and accurate short read alignment with Burrows–Wheeler transform. *Bioinformatics* **25**, 1754–1760 (2009).
31. A. Dobin, C. A. Davis, F. Schlesinger, J. Drenkow, C. Zaleski, S. Jha, P. Batut, M. Chaisson, T. R. Gingeras, STAR: Ultrafast universal RNA-seq aligner. *Bioinformatics* **29**, 15–21 (2013).
32. M. A. DePristo, E. Banks, R. Poplin, K. V. Garimella, J. R. Maguire, C. Hartl, A. A. Philippakis, G. del Angel, M. A. Rivas, M. Hanna, A. McKenna, T. J. Fennell, A. M. Kernytsky, A. Y. Sivachenko, K. Cibulskis, S. B. Gabriel, D. Altshuler, M. J. Daly, A framework for variation discovery and genotyping using next-generation DNA sequencing data. *Nat. Genet.* **43**, 491–498 (2011).
33. S. Hänzelmann, R. Castelo, J. Guinney, GSVA: Gene set variation analysis for microarray and RNA-seq data. *BMC Bioinformatics* **14**, 7 (2013).
34. M. I. Love, W. Huber, S. Anders, Moderated estimation of fold change and dispersion for RNA-seq data with DESeq2. *Genome Biol.* **15**, 550 (2014).
35. A. Subramanian, P. Tamayo, V. K. Mootha, S. Mukherjee, B. L. Ebert, M. A. Gillette, A. Paulovich, S. L. Pomeroy, T. R. Golub, E. S. Lander, J. P. Mesirov, Gene set enrichment analysis: A knowledge-based approach for interpreting genome-wide expression profiles. *Proc. Natl. Acad. Sci. U.S.A.* **102**, 15545–15550 (2005).

Acknowledgments: This work was also performed, in part, by The University of Texas MD Anderson Immunotherapy Platform, and we thank A. Khan (Program Director) and M. Polk (Administrative Director) for assistance. We especially thank all of the patients for participation in this clinical study. **Funding:** These studies were supported, in part, by Bristol Myers Squibb. The research work was also supported by Stand Up To Cancer–Cancer Research Institute Cancer Immunology Dream Team Translational Research Grant SU2CAACR-DT1012 [to J.P.A., P.S., and S.K.S.; Stand Up To Cancer is a program of the Entertainment Industry Foundation administered by the American Association for Cancer Research (AACR)], a Prostate Cancer Foundation (PCF) 2014 Young Investigator Award (to S.K.S.), Cancer Prevention Research in Texas Grant RP120108 (to P.S.), NIH/National Cancer Institute (NCI) Grant R01 CA1633793 (to P.S.), NIH/NCI Award P30CA016672, and The University of Texas MD Anderson Cancer Center Prostate Cancer Moon Shot Program. The Genitourinary Cancers Program of the Cancer Center support grant shared resources at The University of Texas MD Anderson Cancer Center. P.S., and J.P.A. are members of the Parker Institute for Cancer Immunotherapy at The University of Texas MD Anderson Cancer Center. **Author contributions:** S.K.S. was involved in the development of methodology; acquisition, analysis, and interpretation of data; and writing, review, and/or revision of the manuscript. L.V., H.Z., J.B., Q.X., A.R., C.-J.W., and J.Z. were involved in the acquisition, analysis, and interpretation of data. S.S.Y. was involved in the acquisition, analysis, and interpretation of data and writing, review, and/or revision of the manuscript. A.A. was involved in the acquisition of data and writing, review, and/or revision of the manuscript. P.G.C., B.F.C., L.L.P., P. Troncoso, and C.L.L. were involved in the acquisition of data. R.S.T. and P. Thall were involved in the analysis and interpretation of data. A.F. was involved in the development of methodology and acquisition, analysis, and interpretation of data. J.P.A. and P.S. were involved in study supervision; conception and design; development of methodology; acquisition, analysis, and interpretation of data; and writing, review, and/or revision of the manuscript. **Competing interests:** S.K.S. reports consulting, advisory roles, and/or stocks/ownership for Amgen, Apricity Health, AstraZeneca, Bayer, Bristol Myers Squibb, Dava Oncology, Dendreon, Exelixis, Janssen Oncology, and Polaris. J.P.A. reports consulting, advisory roles, and/or stocks/ownership for Achelois, Apricity Health, BioAlta, Codiak BioSciences, Dragonfly Therapeutics, Forty-Seven Inc., Hummingbird, ImaginAb, Jounce Therapeutics, Lava Therapeutics, Lytix Biopharma, Marker Therapeutics, Neon Therapeutics, Polaris, and Tvardi Therapeutics and owns a patent licensed to Jounce Therapeutics. P.S. reports consulting, advisory roles, and/or stocks/ownership for Achelois, Apricity Health, BioAlta, Codiak BioSciences, Constellation, Dragonfly Therapeutics, Forty-Seven Inc., Hummingbird, ImaginAb, Jounce Therapeutics, Lava Therapeutics, Lytix Biopharma, Marker Therapeutics, Neon Therapeutics, Oncolytics, and Polaris and owns a patent licensed to Jounce Therapeutics. **Data and materials availability:** All data associated with this study are present in the paper or the Supplementary Materials. Sequence data have been deposited at the European Genome-phenome Archive under accession number EGAS00001004050.

Submitted 11 September 2019
Accepted 6 March 2020
Published 1 April 2020
10.1126/scitranslmed.aaz3577

Citation: S. K. Subudhi, L. Vence, H. Zhao, J. Blando, S. S. Yadav, Q. Xiong, A. Reuben, A. Aparicio, P. G. Corn, B. F. Chapin, L. L. Pisters, P. Troncoso, R. S. Tidwell, P. Thall, C.-J. Wu, J. Zhang, C. L. Logothetis, A. Futreal, J. P. Allison, P. Sharma, Neoantigen responses, immune correlates, and favorable outcomes after ipilimumab treatment of patients with prostate cancer. *Sci. Transl. Med.* **12**, eaaz3577 (2020).

Science Translational Medicine

Neoantigen responses, immune correlates, and favorable outcomes after ipilimumab treatment of patients with prostate cancer

Sumit K. Subudhi, Luis Vence, Hao Zhao, Jorge Blando, Shalini S. Yadav, Qing Xiong, Alexandre Reuben, Ana Aparicio, Paul G. Corn, Brian F. Chapin, Louis L. Pisters, Patricia Troncoso, Rebecca Slack Tidwell, Peter Thall, Chang-Jiun Wu, Jianhua Zhang, Christopher L. Logothetis, Andrew Futreal, James P. Allison, and Padmanee Sharma

Sci. Transl. Med., **12** (537), eaaz3577.
DOI: 10.1126/scitranslmed.aaz3577

New ideas about neoantigens
Tumors with a low mutational burden are thought to have fewer neoantigens available for T cells to respond to and thus are not necessarily considered for checkpoint blockade therapy. Subudhi *et al.* treated patients with metastatic castration-resistant prostate cancer, which has a relatively low mutation burden, with ipilimumab. Patients who responded to the treatment had a T cell response signature and detectable neoantigen immunity. These results indicate that checkpoint blockade therapy with ipilimumab can instigate T cell responses to tumor neoantigens despite the tumor mutational burden status.

Science Translational Medicine (ISSN 1946-6242) is published by the American Association for the Advancement of Science. 1200 New York Avenue NW, Washington, DC 20005. The title *Science Translational Medicine* is a registered trademark of AAAS.